BECKER, P. J. & COPPENS, P. (1974). *Acta Cryst.* A**30**, 129–147.
BECKER, P. J. & COPPENS, P. (1975). *Acta Cryst.* A**31**, 417–425.
BUTTNER, R. H. (1990). PhD thesis, Univ. of Western Australia, Australia.
CHEN, C. H., KWO, J. & HONG, M. (1988). *Appl. Phys. Lett.* **52**, 841–843.
Commercial Crystal Laboratories Inc. (1991). *Physical Properties of Strontium Titanate*, Company Circular No. 3.
FLEURY, P. A., SCOTT, J. F. & WORLOCK, J. A. (1968). *Phys. Rev. Lett.* **21**, 16–19.
HALL, S. R. & STEWART, J. M. (1989). Editors. *XTAL2.6 Users Manual*. Univs. of Western Australia, Australia, and Maryland, USA.
HIRSHFELD, F. L. (1977). *Isr. J. Chem.* **16**, 198–201.
HUTTON, J., NELMES, R. J. & SCHEEL, H. J. (1981). *Acta Cryst.* A**37**, 917–920.
JAHN, H. A. & TELLER, E. (1937). *Proc. R. Soc. London Ser. A*, **161**, 220–235.
LARSON, A. C. (1970). In *Crystallographic Computing*, edited by F. R. AHMED. Copenhagen: Munksgaard.
MASLEN, E. N. & SPADACCINI, N. (1989). *Acta Cryst.* B**45**, 45–52.
MASLEN, E. N. & SPADACCINI, N. (1992). In preparation.
ROTH, R. S. (1957). *J. Res. Natl Bur. Stand.* **58**, 75–88.
SCHEEL, H. J. (1976). *Z. Kristallogr.* **143**, 417–428.
SCHOOLEY, J. F., HOSLER, W. R. & COHEN, M. L. (1964). *Phys. Rev. Lett.* **14**, 474–475.
SCOTT, J. F. (1974). *Rev. Mod. Phys.* **46**, 86–128.
STIRLING, W. G. (1972). *J. Phys. C*, **5**, 2711–2730.
SUGI, T., HASEGAWA, S. & OHARA, G. (1968). *Jpn. J. Appl. Phys.* **7**, 358–362.
UNOKI, H. & SAKUDO, T. (1967). *J. Phys. Soc. Jpn*, **23**, 546–552.
ZACHARIASEN, W. H. (1969). *Acta Cryst.* A**25**, 102.

Acta Cryst. (1992). B**48**, 644–649

Electron Difference Density and Structural Parameters in $CaTiO_3$

BY R. H. BUTTNER AND E. N. MASLEN

Department of Physics, University of Western Australia, Nedlands 6009, *Australia*

(*Received* 16 *August* 1991; *accepted* 22 *April* 1992)

Abstract

Calcium titanate, $CaTiO_3$, $M_r = 135.98$, orthorhombic, *Pbnm*, $a = 5.388\ (1)$, $b = 5.447\ (1)$, $c = 7.654\ (1)$ Å, $V = 224.63\ (1)$ Å^3, $Z = 4$, $D_x = 4.02$ Mg m^{-3}, λ(Mo $K\alpha$) = 0.71069 Å, $\mu = 5.778$ mm^{-1}, $F(000) = 264$, $T = 298$ K, $R = 0.043$, $wR = 0.028$ for data set (1) and $R = 0.037$, $wR = 0.026$ for data set (2) for 1240 and 1241 unique reflections respectively. Structural parameters and difference electron densities for $CaTiO_3$ were determined from two sets of X-ray diffraction data measured independently. There was close agreement between the analyses. The topography of $\Delta\rho$ near the Ti atom resembles that frequently observed for d^8 or d^9 systems, with a change of sign, indicating that its $3d$ subshell is partly filled. There are indications of slight Jahn–Teller distortion in the structural geometry, in the vibration parameters and in the electron density.

Introduction

The first perovskite mineral $CaTiO_3$ was assigned that name by Gustav Rose in 1830 (Hazen, 1988). Naray-Szabo (1943) determined its structure to be monoclinic but Megaw (1946) pointed out that an orthorhombic cell could be derived from the monoclinic lattice. Single-crystal structure analysis by Kay & Bailey (1957) confirmed the orthorhombic cell, having space group *Pcmn*. The volume of the orthorhombic cell is approximately four times that of an ideal cubic perovskite ($Pm\bar{3}m$ symmetry), and is analogous to tetragonal $KCuF_3$ (Buttner, Maslen & Spadaccini, 1990). Structural parameters for $CaTiO_3$ have been determined accurately by Sasaki, Prewitt, Bass & Schulze (1987).

The electron distributions for ideal cubic KMF_3 perovskites with M = Mn, Fe, Co, Ni and Zn have been studied by Kijima, Tanaka & Marumo (1981, 1983), by Miyata, Tanaka & Marumo (1983) and by Buttner & Maslen (1988). The effect of Jahn–Teller (Jahn & Teller, 1937) distortion of the M atom was examined by Buttner, Maslen & Spadaccini (1990), their results for $KCuF_3$ being broadly consistent with those re-derived from earlier data by Tanaka & Marumo (1982). These studies of the perovskites are now extended to $CaTiO_3$, and thus to the effect on the electron density of structural distortions due to the atomic radii differing from the ideal cubic structure values.

Experimental

Crystals were prepared by the flux-growth method used by Sugi, Hasegawa & Ohara (1968) to crystallize $SrTiO_3$. 10 g of a mixture of $KF:KMoO_4:CaTiO_3$ in the molar ratio 60:30:10 was pressed into a pellet and placed in a platinum crucible with a small quantity of the mixture sealing the gap to a capping crucible. The assembly was heated to 1323 K and

0108-7681/92/050644-06$06.00

cooled at a rate of 15 K h^{-1}. The well-faceted $CaTiO_3$ crystals in the crucible proper were identified by multiple peaks in the diffraction profiles to be multi-domained or twinned, as often occurs in distorted perovskites. One single-domained specimen was extracted from material sealing the gap between the crucibles. The crystal was a parallelepiped with flat (110), ($\bar{1}\bar{1}0$), ($\bar{1}1\bar{3}$), ($\bar{1}13$), ($\bar{2}2\bar{1}$), ($22\bar{1}$) faces and one damaged face satisfactorily approximated by ($\bar{1}0\bar{2}$), spaced 50, 50, 25, 25, 28.5, 28.5 and 40 μm respectively from an origin within the specimen. The measurements are accurate to about 2 μm. There was no evidence of twinning in the diffraction profiles for this specimen. Intensities for Friedel-related reflections agreed closely, notwithstanding that crystal's damaged face. The irregularity has little effect on the absorption factor because of the low absorption coefficient of 5.778 mm^{-1}. Using different crystal orientations two intensity data sets were measured independently on a Syntex $P2_1$ diffractometer. Unit-cell dimensions (for both data sets) were obtained from six reflections ($46.08 \le 2\theta \le 67.71°$). Scan type $\omega/2\theta$. Six standards were measured every 100 reflections. Background measurement made for one-third of the total scan time. $(\sin\theta/\lambda)_{max} = 1.08$ Å^{-1}, $-11 \le h \le 11$, $-11 \le k \le 11$, $-16 \le l \le 16$. Variances in measured structure factors $\sigma^2(F_o)$ from counting statistics were modified for source instability using the program *DIFDAT* (Hall & Stewart, 1989) and increased when necessary by comparing intensities of equivalent reflections following the Fisher test option of the program *SORTRF* (Hall & Stewart, 1989). Full-matrix least-squares refinement with weights $w = 1/\sigma^2(F_o)$ for all independent reflections. That is, following good statistical practice, no reflections were classified arbitrarily as 'unobserved'. To the degree that the value of 0.45 for the index $\sum(F_1 - F_2)^2/\sum\sigma^2(F_1 - F_2)$ is less than 1.0, the $\sigma^2(F_o)$ values are over-estimated and/or errors in the two data sets are correlated. The subscripts denote data-set number. Other experimental and refinement details are given in Table 1.† Atomic form factors and dispersion corrections were taken from *International Tables for X-ray Crystallography* (1974, Vol. IV). Lorentz, polarization and absorption factors evaluated analytically. Least-squares residual $\sum w|F_o - F_c|^2$ minimized by adjusting one scale, seven position and 20 independent vibration parameters, along with r^* for the Zachariasen (1969) isotropic secondary-extinction corrections as formulated by Larson (1970). Final shift/e.s.d. < 0.0001.

† A list of structure factors for data set (2) has been deposited with the British Library Document Supply Centre as Supplementary Publication No. SUP 55166 (6 pp.). Copies may be obtained through The Technical Editor, International Union of Crystallography, 5 Abbey Square, Chester CH1 2HU, England.

Table 1. *Experimental and refinement data for* $CaTiO_3$

	Data set (1)	Data set (2)
Monochromator	Graphite	Graphite
Scan speed (° min^{-1})	6.51	6.51
Peak scan width ($a + b\tan\theta$) (°)	1.70, 0.69	1.75, 0.69
Max. 2θ (°)	100	100
Max. variation in intensity of standards ±600, ±060, ±008 (%)	1.7	1.7
No. of reflections measured	11924	17777
Transmission range in absorption corrections	0.68–0.78	0.68–0.78
R_{int} (before and after absorption)	0.063, 0.057	0.067, 0.061
No. of independent reflections $0 \le 11$, $0 \le 11$, $0 \le 16$	1240	1241
R	0.043	0.037
wR	0.028	0.026
S	3.00 (6)	2.70 (6)
Weights	$1/\sigma^2(F_o)$	$1/\sigma^2(F_o)$
Final max. shift/e.s.d.	0.0002	0.0002
$\Delta\rho_{max}$ (e Å^{-3})	1.4 (2)	1.9 (2)
$\Delta\rho_{min}$ (e Å^{-3})	−1.3 (2)	−1.7 (2)
y_{min} (extinction)	0.88	0.90

The interset indices $\sum|F_1 - F_2|/\sum|F_1 + F_2|$ and $[\sum w(F_1 - F_2)^2/\sum w(F_1 + F_2)^2]^{1/2}$ are 0.016 and 0.011 respectively. Computer programs *STARTX*, *DIFDAT*, *ABSORB*, *ADDATM*, *ADDREF*, *FC*, *SFLSX*, *BONDLA*, *FOURR*, *CHARGE*, *CONTRS*, *SLANT* and *PLOT* from the *XTAL*2.6 system (Hall & Stewart, 1989) installed on a SUN 280 computer, were used in the analysis.

Structural geometry

The atomic coordinates for the two refinements listed in Table 2 agree as closely as expected from the standard deviations, and are also consistent with those of Sasaki, Prewitt, Bass & Schulze (1987). To a close approximation the distortion from the ideal cubic $Pm\bar{3}m$ structure may be described as tilting of the oxygen octahedra surrounding the Ti atoms (Glazer, 1972, 1975). This tilting maintains the *B*—O distance while shortening the *A*—O vectors, as required for *A* radii smaller than the ideal value for the cubic ABO_3 structure. An equivalent cubic $CaTiO_3$ cell would have $a_{eq} = (V/4)^{1/3} = 3.830$ Å. The corresponding Ti—O distance of 1.915 Å would be less than the value of 1.9552 (4) Å for $SrTiO_3$ and the average value of 2.008 Å in $BaTiO_3$ (Buttner, 1990). However, in the orthorhombic $CaTiO_3$ structure the average Ti—O bond length of 1.957 (1) Å is close to that in $SrTiO_3$.

Relevant interatomic distances for data set (2) are listed in Table 3. Assuming that the Ca—O bond lengths in $CaTiO_3$ should be shorter than the corresponding Sr—O bond length of 2.7651 Å in $SrTiO_3$, the Ca—O distances indicate that eight O atoms coordinate with Ca, compared with 12 for the ideal perovskite structure. The irregular geometry for the Ca—O coordination is shown in Fig. 1(*a*). The Ti

Table 2. *Positional and anisotropic thermal parameters* ($U \times 10^5$ Å^2) *for* $CaTiO_3$

$T = \exp[-2\pi^2(a^{*2}h^2U_{11} + b^{*2}k^2U_{22} + c^{*2}l^2U_{33} + 2a^*b^*hkU_{12} + 2a^*c^*hlU_{13} + 2b^*c^*lkU_{23})]$. Results are given as data set (1)/data set (2) with results for the first analysis followed by those for the second for each table entry.

	x	y	z	U_{11}	U_{22}	U_{33}	U_{12}	U_{13}	U_{23}
Ti	0.00	0.50	0.00	585 (9)	566 (8)	427 (7)	−4 (8)	14 (8)	26 (5)
	0.00	0.50	0.00	590 (7)	556 (6)	423 (4)	−4 (7)	8 (6)	28 (4)
Ca	−0.00629 (7)	0.03393 (6)	0.25	814 (11)	907 (10)	871 (9)	−161 (11)	0	0
	−0.00626 (6)	0.03410 (5)	0.25	788 (9)	905 (8)	849 (8)	−159 (9)	0	0
O1	0.0707 (3)	0.4842 (2)	0.25	918 (44)	1072 (42)	352 (30)	−72 (3)	0	0
	0.0704 (2)	0.4842 (2)	0.25	935 (37)	1019 (34)	358 (27)	−70 (26)	0	0
O2	0.7109 (1)	0.2884 (1)	0.0370 (1)	726 (29)	735 (25)	905 (24)	−259 (23)	49 (24)	−114 (22)
	0.7109 (1)	0.2884 (1)	0.0369 (1)	725 (22)	683 (21)	916 (23)	−231 (19)	59 (20)	−87 (19)

Table 3. *Interaction vector lengths* (Å) *for* $CaTiO_3$ *data set* (2)

Superscripts indicate multiplicity.

Vectors

	Ti		O1		O2	
Ca	3.1785 (5)^2	3.3370 (5)^2	2.364 (1)^1	3.024 (1)^1	2.3804 (8)^2	3.2312 (8)^2
	3.2821 (5)^2	3.4823 (5)^2	2.486 (1)^1	3.052 (1)^1	2.6268 (8)^2	
					2.6696 (8)^2	
Ti	3.8268 (5)^2	3.8308 (5)^4		1.9525 (4)^2	1.9582 (7)^2	1.9594 (7)^2

O—Ti—O octahedral angles (°)

O1—Ti—O2	89.26 (4)
O1—Ti—O2	89.62 (2)
O2—Ti—O2	89.42 (2)
O1—Ti—O1 = O2—Ti—O2^2	180 by symmetry

atom, on the other hand, is at the centre of a near-perfect octahedron as indicated by the small variation in Ti—O lengths and the O—Ti—O angles which are within 1° of 90 or 180°. Although the differences between the Ti—O bond lengths are small it is not obvious why the O1—Ti—O1 vectors should contract relative to both O2—Ti—O2 vectors.

Atomic vibrations

The vibrational parameters for the two refinements listed in Table 2 are also consistent within the standard deviations, and agree broadly with the U_{ij} values deposited by Sasaki, Prewitt, Bass & Schulze (1987), although there are significant differences in detail. Typical are those authors' values of $U_{11} = 800\,(50)$, $U_{22} = 840\,(50)$, $U_{33} = 370\,(40)$ and $U_{12} = 10\,(40) \times 10^{-5}$ Å^2 for O1. The low U_{33} values for Ti and O1 indicate that the structure is tightly packed along the O1—Ti—O1 vectors. For the Ti—O2 vector displaced from the $z/c = 0$ plane, the transformed U_{ij} for O2 along the bond is $499\,(21) \times 10^{-5}$ Å^2. That is, both O1 and O2 vibrate less strongly than Ti in the Ti—O directions. This is consistent with the corresponding Ti—O vibrational motion in $SrTiO_3$ reported by Buttner & Maslen (1992). The mean-square amplitudes for Ti are significantly less than those for Ca, as expected from the rigid Ti—O geometry.

Atomic charges

Atomic charges, determined by projecting the difference density onto atomic density basis functions following the method of Hirshfeld (1977) are listed in Table 4. The signs of the charges are consistent with electronegativities for all the atoms in the structure. The charges from the two independent measurements agree closely except for Ca, where the difference approaches 2σ. Nevertheless the larger cation charges for data set (2) are consistent with a general trend in charges measured for perovskite structures – namely the electron count on the heavier atoms increases with the extinction correction $1/y$. The sensitivity of the charges to the extinction correction is shown by the charges evaluated from data

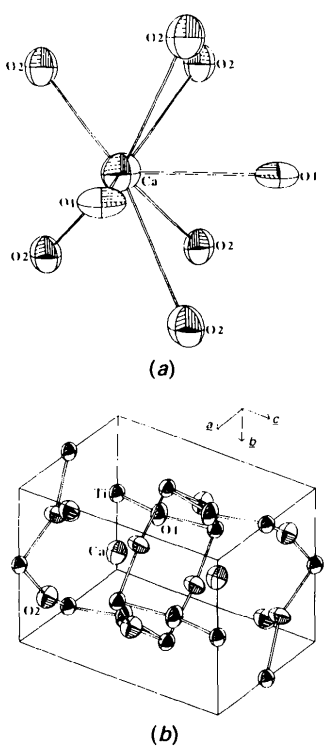

Fig. 1. (*a*) Ca coordination and (*b*) cell structure for $CaTiO_3$. Vibrational ellipsoids at 95% probability level.

Table 4. *Atomic charges* (e) *based on Hirshfeld partitioning and IAM*

	Data set (1)	Data set (2)	Data set (2) (no extinction correction)
Ti	0.58 (5)	0.59 (4)	0.90 (4)
Ca	0.47 (5)	0.56 (4)	0.95 (4)
O1	−0.28 (4)	−0.29 (4)	−0.59 (4)
O2	−0.39 (4)	−0.43 (4)	−0.67 (4)

set (2) assuming that no extinction correction is warranted, listed in the last column of Table 4.

Even the extreme assumption of no extinction gives charges with magnitudes less than the formal oxidation-state values. Although differences between the negative charges on O1 and O2 for the two analyses are barely significant those differences are correlated with the Ca charge. Six of the eight atoms closest to Ca are O2. That is, if Ca is eight coordinated as described above, the O2:O1 ratio in the first coordination sphere is 3:1, compared with the cell-content ratio of 2:1. The charge on O2 is more negative than that on O1. The geometrical distortion maximizes the number of interactions between the Ca atom and the more negatively charged O2 atom. This suggests that the Ca position is influenced by Coulomb energy considerations, acting cooperatively with tilting of the Ti—O octahedra in the rearrangement from the ideal structure.

Because the values obtained assuming no extinction appear physically reasonable one cannot assert with confidence that charges determined by least-squares minimization of structure-factor differences are more reliable. The development of improved corrections for extinction which are independent of the structure refinement is necessary.

Difference density

The $CaTiO_3$ cell shown in Fig. 1(*b*) resembles that of the Jahn–Teller-distorted $KCuF_3$ structure [see Fig. 1 of Buttner, Maslen & Spadaccini (1990)]. The *c* axis is doubled and the transition metal is tightly packed along the [001] direction in both cases. Difference density sections for $CaTiO_3$ were compared with the corresponding sections for $KCuF_3$. For the orthorhombically distorted $CaTiO_3$ structure some atoms are slightly displaced from the ideal planes. In the figures, italic lettering distinguishes those atoms from exactly coplanar atoms which are identified by bold type. As indicated by the (100) plane shown in Figs. 2(*a*) and 2(*b*), the maps for both data sets agree closely. The marked concentration of density along the Ti—O1 and Ti—O2 vectors contrasts with the depletion of density along the corresponding vectors in $KCuF_3$. The (001) plane shown in Fig. 3(*a*) has near-to-fourfold symmetry near the Ti atom, with the characteristic depletion at the structural cavity marked *X* having a minimum value of -0.7 e Å^{-3}. Similar approximate symmetry occurs in the $KCuF_3$ structure.

The approximate fourfold symmetry of the positive density in Fig. 3(*a*), containing the two independent Ti—O2 vectors, contrasts with the marked anisotropy of the orthogonal (110) section containing the Ti—O1 vector shown in Fig. 3(*b*). There is pronounced depletion of density near Ti along the Ti—Ca vectors corresponding to the [111] lobes which would be maximally occupied by t_{2g} orbitals for 3*d* electrons. The topography of the density near the Ti atom in Figs. 2(*a*) and 2(*b*) resembles that frequently observed in Cu and Ni structures, except that the sign of the density is reversed. This is evident by comparing the (001) plane for $CaTiO_3$ shown in Fig. 3(*a*) with Fig. 3(*a*) for $KCuF_3$ (Buttner, Maslen & Spadaccini, 1990), or

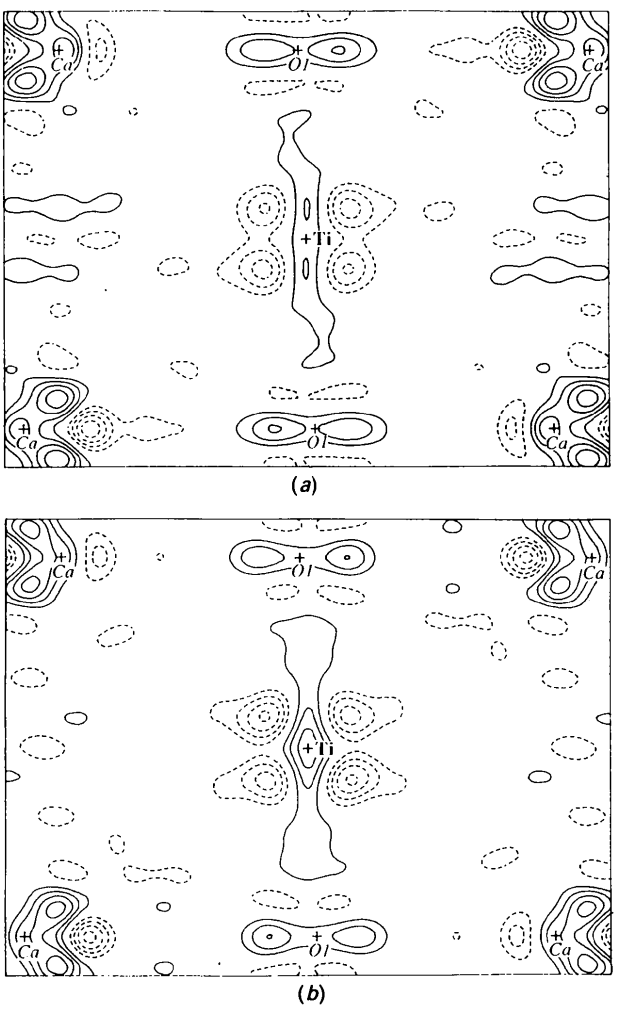

Fig. 2. $\Delta\rho$ for $CaTiO_3$, (100) plane: (*a*) data set (1), (*b*) data set (2). Map borders 6.2 × 4.6 Å. Contour intervals 0.4 e Å^{-3}, positive contours solid, negative contours dashed.

by comparing the (100) plane for $CaTiO_3$ shown in Fig. 2(*b*) with the analogous section in Fig. 4(*d*) for $KNiF_3$ (Maslen & Spadaccini, 1989).

The difference density minimizes along the Ti—Ca vectors about 0.55 Å from the Ti nucleus, *i.e.* about 0.05 Å further than the distance from the t_{2g} maxima and e_g minima to the Ni nucleus in $KNiF_3$, and 0.11 Å further than that from the corresponding minima to the Yb nucleus in $[Yb(H_2O)_9](CF_3SO_3)_3$ (Chatterjee, Maslen & Watson, 1988). It has been conjectured that such features could be anharmonic and not electronic in origin, because of their proximity to the nuclei and the statistical significance of a high-order cumulant if the corresponding coefficient is determined by least-squares refinement of X-ray diffraction data.

Neither proximity to a nucleus nor the statistical significance of a cumulant determined from data with limited resolution is sufficient to confirm that a given feature in an X-ray difference density is anharmonic, as most theoretically calculated deformation densities contain sharp features close to the stationary nuclei. The corresponding Fourier coefficients may well resemble those arising from anharmonic vibrational motion.

To differentiate anharmonicity from sharp electronic features reliably requires additional information such as that provided by neutron diffraction for simple cases where anharmonic effects are large, such as BaF_2 (Cooper, Rouse & Willis, 1968). However, neutron diffraction is limited in power by the low neutron fluxes available, and becomes progressively less useful as the complexity of structures increases and their scattering power declines.

It may be possible to assess whether features in X-ray difference maps are electronic or anharmonic from X-ray measurements at two temperatures. Anharmonic components in $\Delta\rho$ should not increase in size as the temperature is lowered. Electronic effects are unlikely to increase as the temperature is raised. Another indicator is the Bragg angle of the contribution to the structure factors from a difference density feature. The contribution of an nth-order cumulant to the structure factor should vary as the product of the scattering and the temperature factors, multiplied by the $(n-1)$th power of $\sin\theta/\lambda$.

The origin of X-ray difference density features for $[Yb(H_2O)_9](CF_3SO_3)$ was investigated by Imerito (1987), who repeated the original room-temperature data measurements at 120 K. The $\Delta\rho$ depletions near the Yb nucleus deepened, from -3.2 to -5.5 e Å^{-3}, as the minima moved to within 0.37 Å of the nucleus at the lower temperature. This change in $\Delta\rho$ topography near the Yb—O bond is consistent with exchange depletion of the electron density in closed subshells near the nucleus increasing as the Yb—O distance contracts. The study confirmed conclusions from a neutron study of the isomorphous rare-earth triflate $[Nd(H_2O)_9](CF_3SO_3)$, which gave no indication of anharmonicity affecting the diffraction data. Equivalent results have been obtained for the ideal perovskite $KZnF_3$ and for K_2SiF_6 from studies at two temperatures (Maslen, 1992).

The $(\sin\theta/\lambda)_{max}$ of 1.08 Å^{-1} for $CaTiO_3$ is larger than the value of 0.95 Å^{-1} for $[Yb(H_2O)_9](CF_3SO_3)$, but the t_{2g} minima are further from the nuclei than the corresponding minima in the rare-earth triflates. As those minima also deepen less rapidly with increased $(\sin\theta/\lambda)_{max}$ than is expected for anharmonic terms, it is unlikely that they are anharmonic in nature.

The density near the Ti atom in the (110) plane, shown in Fig. 3(*b*), has strongly developed mirror symmetry relating the densities along the two non-equivalent Ti—O2 contacts. Because the two non-

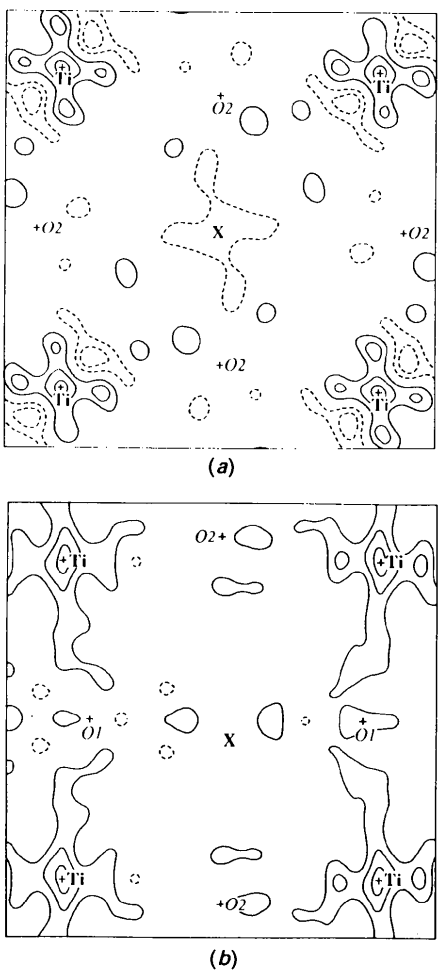

Fig. 3. $\Delta\rho$ for $CaTiO_3$: (*a*) (001) plane, *a* axis diagonal bottom left to top right; (*b*) (110) plane. Map borders 5.2 × 5.2 Å. Contouring as in Fig. 2.

equivalent Ti—O2 vectors have closely similar lengths, the net force on the nucleus in the promolecule model for the structure is small. For this reason little polarization of the density close to the nucleus is expected. The gradient of the electron density near the O2 nucleus is close to zero.

The electron density at the Ca nucleus is 0.8 e $Å^{-3}$. The geometry of the electron density near the nucleus is unsymmetrical, as expected from the irregular Ca coordination. There is a trend towards electron depletion *ca* 0.3 Å from the nucleus along the Ca—O bonds, but the magnitude of that depletion does not correlate with Ca—O bond length. One obvious trend is the orientation of the 1.6 e $Å^{-3}$ high electron density lobes away from Ca—O bonds and the shorter Ca—Ti contacts. Those lobes define a figure which is as irregular as the Ca-atom coordination. Their orientation is consistent with electron transfer from regions where the Ca atom overlaps strongly with its neighbours towards regions where no strong overlap occurs. A more detailed study shows that the topography of the density nearer the Ca nucleus is consistent with the requirements of structural stability for the Ca atom.

Electronic state of Ti

Elementary descriptions of the alkaline-earth titanates are based on an ionic model assuming Ca^{2+}, Ti^{4+} and O^{2-} states. That model must be modified if it is to account for the small differences in Ti—O1 and Ti—O2 lengths, the differences between the vibrational amplitudes for O1 and O2, and the marked anisotropy of $\Delta\rho$ near the Ti nucleus.

In an ideal Ti^{4+} state the $3d$ subshell is empty. The sign reversal of the Ti density in $CaTiO_3$ compared with that for a transition metal with a nearly-full $3d$ subshell reflects an electron/hole relationship between these two situations. The topography of $\Delta\rho$ strongly suggests that the $3d$ subshell is partly occupied. Noting that a $3d^1$ configuration would be Jahn–Teller unstable, we first seek confirmation of Jahn–Teller distortion in the structural geometry. The Ti—O1 bond is 0.0062 (6) Å shorter than the mean Ti—O2 distance of 1.9588 (5) Å. The vibrational characteristics for the Ti, O system are also consistent with a $3d^\delta$ state for the Ti atom, as Ti vibrates anisotropically, and more strongly than either O1 or O2 along the short Ti—O bonds. It would be difficult to conclude that this effect is real from the structural parameters, without the much stronger evidence in the topography of the difference density.

The contributions of computer programs by their authors, R. Alden, G. Davenport, R. Doherty, W. Dreissig, H. D. Flack, S. R. Hall, J. R. Holden, A. Imerito, R. Merom, R. Olthof-Hazekamp, M. A. Spackman, N. Spadaccini and J. M. Stewart to the *XTAL*2.6 system (Hall & Stewart, 1989), used extensively in this work, is gratefully acknowledged. This research was supported by the Australian Research Council.

References

BUTTNER, R. H. (1990). PhD thesis, Univ. of Western Australia, Australia.
BUTTNER, R. H. & MASLEN, E. N. (1988). *Acta Cryst.* C**44**, 1707–1709.
BUTTNER, R. H. & MASLEN, E. N. (1992). *Acta Cryst.* B**48**, 639–644.
BUTTNER, R. H., MASLEN, E. N. & SPADACCINI, N. (1990). *Acta Cryst.* B**46**, 131–138.
CHATTERJEE, A., MASLEN, E. N. & WATSON, K. J. (1988). *Acta Cryst.* B**44**, 386–395.
COOPER, M. J., ROUSE, K. D. & WILLIS, B. T. M. (1968). *Acta Cryst.* A**24**, 484–493.
GLAZER, A. M. (1972). *Acta Cryst.* B**28**, 3384–3392.
GLAZER, A. M. (1975). *Acta Cryst.* A**31**, 756–762.
HALL, S. R. & STEWART, J. M. (1989). Editors. *XTAL*2.6 *Users Manual*. Univs. of Western Australia, Australia, and Maryland, USA.
HAZEN, R. M. (1988). *Sci. Am.* pp. 52–61.
HIRSHFELD, F. L. (1977). *Isr. J. Chem.* **16**, 198–201.
IMERITO, A. (1987). MSc thesis, Univ. of Western Australia, Australia.
JAHN, H. A. & TELLER, E. (1937). *Proc. R. Soc. London Ser. A*, **161**, 220–235.
KAY, H. F. & BAILEY, P. C. (1957). *Acta Cryst.* **10**, 218–226.
KIJIMA, N., TANAKA, K. & MARUMO, F. (1981). *Acta Cryst.* B**37**, 545–548.
KIJIMA, N., TANAKA, K. & MARUMO, F. (1983). *Acta Cryst.* B**39**, 557–561.
LARSON, A. C. (1970). In *Crystallographic Computing*, edited by F. R. AHMED. Copenhagen: Munksgaard.
MASLEN, E. N. (1992). Private communication.
MASLEN, E. N. & SPADACCINI, N. (1989). *Acta Cryst.* B**45**, 45–52.
MEGAW, H. D. (1946). *Proc. Phys. Soc. London*, **58**, 133–152.
MIYATA, N., TANAKA, K. & MARUMO, F. (1983). *Acta Cryst.* B**39**, 561–564.
NARAY-SZABO, S. (1943). *Naturwissenschaften*, **31**, 203.
SASAKI, S., PREWITT, C. T., BASS, J. D. & SCHULZE, J. D. (1987). *Acta Cryst.* C**43**, 1668–1674.
SUGI, T., HASEGAWA, S. & OHARA, G. (1968). *Jpn. J. Appl. Phys.* **7**, 358–362.
TANAKA, K. & MARUMO, F. (1982). *Acta Cryst.* B**38**, 1422–1427.
ZACHARIASEN, W. H. (1969). *Acta Cryst.* A**25**, 102.